JEE Journal of Ecological Engineering

Journal of Ecological Engineering, 2025, 26(7), 381–393
https://doi.org/10.12911/22998993/203698
ISSN 2299–8993, License CC-BY 4.0

Received: 2025.03.24
Accepted: 2025.04.30
Published: 2025.05.15

Optimization of hexavalent chromium biosorption onto Arabica-coffee waste using response surface methodology

Carmencita Lavado-Meza[1*], Miguel Fernandez-Pezua[2], Leonel De la Cruz-Cerrón[3], Julio Angeles-Suazo[1], Leticia Leiva-Arauco[2], Carmen Lavado-Puente[2], Gregorio Cisneros-Santos[4], Nataly Angeles-Suazo[5], Juan Z. Dávalos-Prado[6]

[1] Universidad Nacional Autónoma de Tayacaja Daniel Hernández Morillo, Facultad de Ingeniería, Tayacaja, Perú
[2] Universidad Nacional Intercultural de la Selva Central Juan Santos Atahualpa, Facultad de Ingeniería, Chanchamayo, Perú
[3] Universidad Continental, Facultad de Ingeniería, Huancayo, Perú
[4] Universidad Nacional Intercultural de la Selva Central Juan Santos Atahualpa, Facultad de Administración de empresas y Negocios Internacionales, Chanchamayo, Perú
[5] Universidad Tecnológica del Perú, Facultad de Ingeniería de Sistemas e Informática, Huancayo, Perú
[6] Instituto de Química Física "Blas Cabrera", Madrid, Spain
* Corresponding author's e-mail: carmencitalavado@unat.edu.pe

ABSTRACT

Face centered cube central composite design (FCCCCD) methodology was applied to optimize the Cr(VI) adsorption capacity of Arabica-coffee pulp biomass (WAC), q_e, as a function of key-factors, such as pH, chromium concentration C_0 and WAC-dose. The quadratic dependence of q_e, with the considered factors, has shown a strong influence of pH. The optimal conditions found in this way were pH 2; C_0 = 75 mg/L and WAC-dose= 0.5 g/L. The characterization of WAC, performed by FTIR and SEM/EDX, allowed the identification of OH, CH, CO, COH functional groups and also showed significant changes, particularly on WAC surface morphology, after biosorption. The experimental isotherm data (q_e *vs* C_e) was well-fitted to three models: Langmuir, Freundlich and Temkin. Furthermore, thermodynamic and kinetic results showed that Cr(VI) biosorption using WAC is an endothermic and spontaneous reaction, following *pseudo*-2nd order kinetics. Finally, this work shows the feasibility of effectively using coffee biomass-waste, a low-cost material, for chromium removal in contaminated aqueous media.

Keywords: optimization Cr(VI) biosorption, agricultural waste, arabica-coffee, isotherm, kinetic.

INTRODUCTION

Fresh water is a scarce resource on our planet, constituting only 3% of water resources, of which only 0.01% is available for human consumption (Nasir et al., 2023). With population growth and industrialization, water can be used in various industrial processes and domestic consumption, which unfortunately are often discharged into surrounding ecosystems without any or poor treatment. These discharges generally include, among others, metals and metalloids (Soon et al., 2022). Heavy metals (Cr^{6+}, Pb^{2+}, Cd^{2+}, Zn^{2+}, Ni^{2+} and Hg^{2+}) and metalloids (e.g. As^{3+}) are toxic, persistent and cause serious damage to both ecosystems and living organisms (Baby et al., 2023; Senanu et al., 2023).

Manufacturing facilities across various sectors rely on chromium as a key material - from fabric production and metal treatment to glassmaking and leather processing. This element also plays vital role in electroplating operations, timber preservation methods, and the creation of colorants (Wang et al., 2023). Compared to compounds containing Cr(III), those including Cr(VI) are toxic and dangerous (Wang et al., 2023), given that

the presence of Cr(VI) in our organism can cause cell death, DNA damage, and liver and kidney dysfunction (Shan et al., 2020). Harmful Cr(VI) easily migrates in water and its contamination can spread widely. Therefore, World Health Organization standards set a very low limit for its concentration (≤ 0.1 mg/L) in various types of water, including drinking water (Khalfaoui et al., 2024). Consequently, reducing of hexavalent chromium concentrations in aqueous matrices represents a critical environmental and public health imperative, given its profound implications for the well-being and biological integrity of ecosystems and organisms (Li et al., 2021).

There are a wide variety of methods to reduce or eliminate the presence of Cr(VI) in aqueous media, e.g. photocatalytic-reduction, precipitation, membrane treatment, electrolysis, adsorption, and others (Li et al., 2021; Shan et al., 2020; Wang et al., 2023). Several of them are often expensive, require strict pretreatment standards, involve high energy consumption, and, above all, produce harmful secondary pollutants (Jimenez-Paz et al., 2023; Solis et al., 2023). In contrast, an excellent alternative is the biosorption method, which uses non-living biological material (biomass). It is an economical, ecological, and effective approach to removing heavy metals (Shan et al., 2020). Biomass from plant residues and those from agro-industrial processes is relatively abundant, inexpensive and contains polymeric compounds, *e.g.* cellulose, hemicellulose, pectin, lignin and proteins, with functional groups that promote the capture of metals (Amaku et al., 2021; Pant et al., 2022; Thangagiri et al., 2022). In this context, the literature reports several waste-biomasses for chromium removal, e.g. *Azadirachta indica* (Thangagiri et al., 2022), nut leaf sheath (Pant et al., 2022), *Arundo donax* stem (Bhattarai et al., 2022), cocoa shell (Pérez et al., 2020), *Eichhornia crassipes* (Tejada et al., 2020), eucalyptus bark and moringa pods (Matouq et al., 2021), *Pentaclethra macrophylla* (Amaku et al., 2021), rice-husk (Lala et al., 2023), among others.

Agricultural trade on a global scale is significantly influenced by coffee, which ranks among the most crucial farming commodities (Freitas et al., 2024). Coffee waste is generated during the production of coffee beans, with pulp being the first by-product (Castillo et al., 2021). Peru produces coffee in 10 regions, with an area of approximately 350 MHa (Alvarado et al., 2022), generating a considerable volume of residues, which represent low-cost and easily accessible material to be used as a potential biosorbent of heavy metals (Collazo-Bigliardi et al., 2019; Dev et al., 2024).

The metal biosorption capacity of biomass depends on numerous factors (e.g. pH, biosorbent dose and concentration, etc.) and these are usually optimized individually (Lu et al., 2023). The process is repeated for the other factors until the optimal biosorption conditions are determined (Rzig et al., 2021). However, this procedure may be inefficient due to the considerable number of experiments required (Boddu et al., 2023). A good alternative to optimize these factors is the response surface methodology (RSM) with central composite design (RSM-CCD), which is an empirical statistical technique that evaluates the simultaneous effects of multiple factors, thereby providing efficient experimental designs (Thakur et al., 2023). RSM-CCD methodology has been successfully employed in the Cr(VI) removal studies using biomasses other than coffee waste (Bayuo et al., 2020; Ben Khalifa et al., 2019; Boddu et al., 2023; Najafpour et al., 2020).

In this work, response surface methodology - face centered cube central composite design (RSM-FCCCCD) was applied to optimize the Cr(VI) adsorption capacity of Arabica coffee-waste (WAC), taking into account important biosorption factors, such as pH, chromium concentration (C_0) and WAC-dose.

METHODS AND MATERIALS

Preparation and characterization of the WAC biosorbent

By-products from coffee processing were collected in Satipo, in Junín, Peru. The collected material was washed using distilled water, followed by heat treatment at 70 °C for two days. The dried substance was then reduced to smaller particles and passed through a N° 70 sieve (Lavado-Meza et al., 2023b). The structural and morphological features of the samples were analyzed by FTIR and SEM/EDX techniques, and evaluations were performedboth before and after the biosorption tests.

Biosorption experiments

Sequential tests were performed using $K_2Cr_2O_7$ solutions in a range of Cr(VI)

concentrations (C_0) from 25 to 75 mg/L. The WAC-dose range considered was 0.5–1.5 g/L, while the pH was modified at the range of 2 to 6 by adding 0.01 M HNO_3 or 0.01 M NaOH and then stirring at 300 rpm for 2 h, followed by filtration to separate the WAC material. Chromium concentrations were determined by diphenylcarbazide methodology (ASTM D1687-02 (2007)), which uses the intensity of the red-purple color for identification and measurement. A Shimadzu UV-1900i spectrophotometer measured the absorbance at λ= 540 nm. The Cr(VI) biosorption capacity of WAC (q_e) was determined Equation 1 in terms of initial-concentration (C_0) and equilibrium-concentration (C_e) of hexavalent chromium; volume of solution (V) and WAC-mass (M).

$$q_e = \frac{(C_0 - C_e)}{M} \times V \quad (1)$$

Optimization of WAC biosorption capacity

Optimization of q_e, expressed as a function of key factors controlling Cr(VI) biosorption, was performed using RSM in Design-Expert 13 software. RSM-FCCCCD methodology was chosen to model, optimize and analyze the effect of three factors: pH, WAC-dose and Cr(VI) concentration, C_0. The highest, medium and lowest values of these factors were labeled with (+1), (0) and (–1), respectively (see Table 1). The design involved 16 runs (8 factorial points, 6 axial points centered on the faces and 2 replicates at the central point). All experimental determinations were replicated in triplicate and q_e was set as the response variable.

Kinetics and equilibrium results

Equilibrium (isotherm) and kinetic studies of Cr(VI) biosorption with WAC were carried out considering optimal conditions of key factors obtained from RSM-FCCCCD methodology. The experimental data were fitted by applying models described below.

Thermodynamic study

Gibbs energy (ΔG^0) of the biosorption process was calculated by Equation 2, while enthalpy (ΔH^0) and entropy (ΔS^0) were evaluated using of Van der Walls equation (Equation 3). The equilibrium constant K_c, at temperature T, was determined as the ratio of Cr(VI) concentration in biosorbent (C_{es}) and in solution (C_e).

$$\Delta G^0 = -RT\, ln(K_c) \quad (2)$$

$$ln(K_c) = \frac{\Delta S^0}{R} - \frac{\Delta H^0}{RT} \quad (3)$$

RESULT AND DISCUSSION

Biosorbent characterization

FTIR spectra of samples, both unloaded (clean) and Cr(VI)-loaded, are shown in Figure 1. FTIR of clean-WAC (See Fig. 1 in blue) exhibits bands related to, i/ (at 3290.83 cm^{-1}) OH groups in cellulose, hemicellulose or lignin (Datt et al., 2022); ii/ (at 2919.83 cm^{-1}) typical C–H vibrations (Suganya et al., 2019); iii/ (at 2363.33 cm^{-1}) alkyne (C≡C) or cyanide (C≡N) groups (Banchhor et al., 2021); iv/ (at 1640.22 cm^{-1}) carbonyl (C=O) groups (Mahmoud et al., 2020); v/ (at 1540.9 cm^{-1}) C=C vibrations in aromatic structures of lignins (Rzig et al., 2021); vi/ (at 1027.90 cm^{-1}) C–O vibrations inside glycosidic linkages of polysaccharides, such as galactomannans and arabinogalactans (Ballesteros et al., 2014).

FTIR of (WAC+Cr) (See Fig.1 in red) displays similar bands to those observed for clean-WAC, but with position shifts and intensity variations; which would reflect the presence of biosorbed Cr(VI) on WAC (Datt et al., 2022; Yusuff et al., 2023). SEM images and EDX diagrams of WAC, unloaded and Cr(VI)-loaded, are depicted in Figure 2. We can see, in Figure 2a, a rough and porous morphology of clean-WAC, typical in organic waste (Murthy and Gowrishankar, 2020). After contact with chromium, the morphology of biosorbent (WAC+Cr) undergoes a drastic transformation, exhibiting a

Table 1. Levels of experimental factors to be used with RSM-FCCCCD methodology

Levels	pH	Dose (g/L)	C_0 (mg/L)
–1	2	0.5	25
0	4	1	50
+1	6	1.5	75

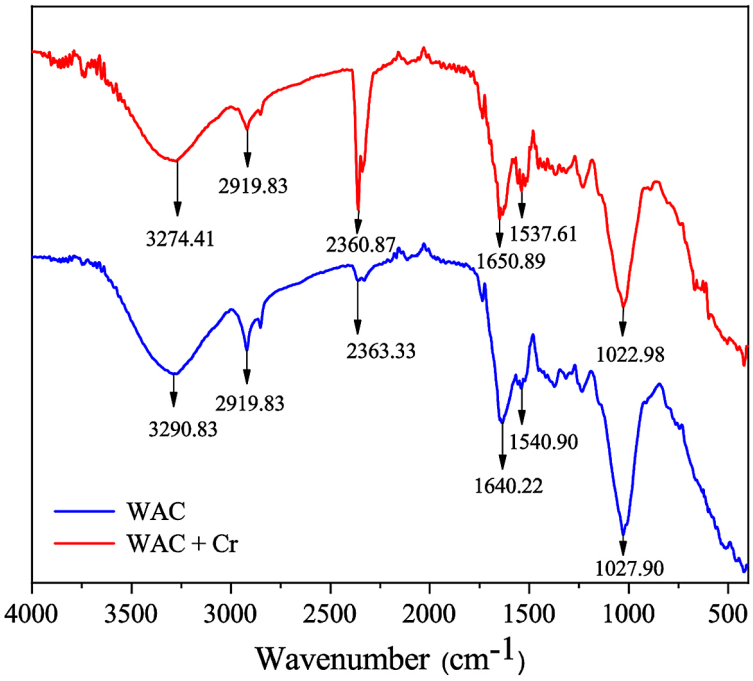

Figure 1. FTIR of WAC, clean or unloaded (blue) and Cr(VI)-loaded (red), at T = 20 °C and contact time, t_{sp} = 120 min

significantly more compact and less porous surface (Fig. 2b), which reflects the impact of chromium biosorption on WAC. EDX diagram of clean-WAC shows a structure including elements such as C, N, and O (see Fig. 2a right), which is consistent with the organic structure of biowaste (Jaihan et al., 2022). The EDX profile of the Cr-loaded WAC also exhibits characteristic Cr peaks (see Fig. 2b right), confirming the incorporation of this metal into the WAC substrate.

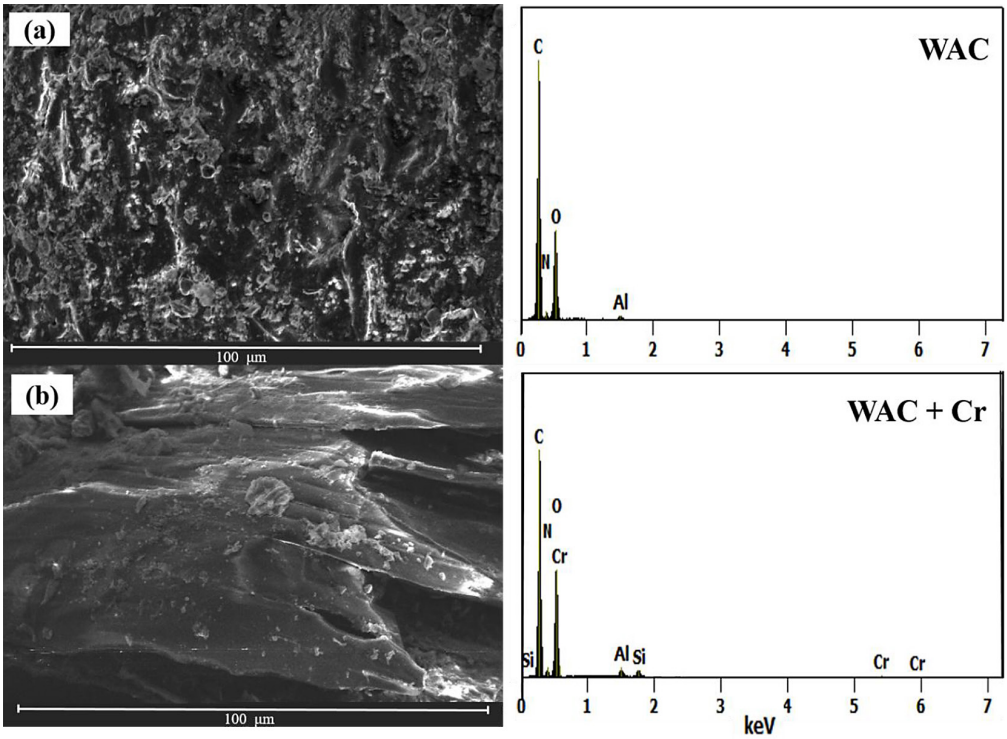

Figure 2. SEM/ EDX profiles of WAC: clean (a) and Cr(VI)-loaded (b)

Optimization of q_e

Table 2 shows the RSM-FCCCD matrix that allows optimizing the relationship of the response function q_e and independent biosorption factors pH, WAC-dose and C_0, represented respectively by, A, B, and C.

Table 3 contains the regression coefficients of the proposed RSM-FCCCD predictive model. The quadratic expression for the predicted Cr(VI) adsorption capacity, $q_{e,p}$ (Equation 4) was identified as the most suitable (R^2 and adjusted $R^2 > 0.9$) to describe the Cr(VI) biosorption process onto WAC.

$$q_{e,p} = 34.7121 - 17.3144A - 2.3313B + 0.4035C + 1.0258AB - 0.0502AC - 0.0430BC + 1.8814A^2 - 0.9750B^2 - 0.0009C^2 \quad (4)$$

Based on the ANOVA results, the significance of each term is established by its p- and F-values. A term is considered statistically significant if $p < 0.05$ (Jaihan et al., 2022; Singh and Bhateria, 2020). In this analysis, the terms A, C, AC, A^2 were found to be significant, while B, AB, BC, B^2, and C^2 were deemed insignificant (Table 4). Notably, the F–value for A (=145.25) is substantially higher than those for B (=3.50) and C (=6.98), indicating that A (pH) exerts the greatest influence among the evaluated parameters. After eliminating the non-significant terms, Equation 4 would be simplified to Equation 5, where the parameters of the two critical factors (pH and C_0) are highlighted.

$$q_{e,p} = 34.7121 - 17.3144A + 0.4035C - 0.0502AC + 1.8814A^2 \quad (5)$$

Interdependence of biosorption factors

The dependence of operational factors (pH, WAC-dose and C_0) on the projected chromium(VI) uptake capacity ($q_{e,p}$) are represented through RSM-FCCCD plots, as depicted in Figure 3. An increasing trend in ($q_{e,p}$ *vs* C_0) is observed in Figures 3a and 3c. Conversely, decreasing trends in (q_{ep} *vs* dose and pH) are evident in Figures 3b and 3c. The increase in $q_{e,p}$ with C_0 can be mainly attributed to the enhanced mass gradient between the solution and the biosorbent, which would act as a driving force transporting chromium to the biosorbent surface (Gupta et al., 2013).

As seen in the previous section, pH exerts a strong influence on Cr(VI) biosorption. Thus, Figures 3b and 3c, show the sharp decrease in $q_{e,p}$ with increasing pH. This finding suggests that strongly acidic pH levels favor Cr(VI) biosorption. Cr(VI), depending on its concentration and

Table 2. FCCCD matrix of the combination of independent factors (pH, WAC-dose, C_0) and dependent or response function q_e

Nº Run	Levels			Independent variables			Response function, q_e (mg/g)	
	A	B	C	pH	C_0 (mg/L)	Dose (g/L)	Experimental	Predicted, $q_{e,p}$
1	1	1	1	6	75	1.5	0.25	0.25
2	1	–1	1	6	75	0.5	2.17	1.00
3	–1	1	1	2	75	1.5	17.61	17.60
4	–1	–1	–1	2	25	0.5	12.91	13.68
5	–1	0	0	2	50	1	18.85	17.01
6	1	0	0	6	50	1	0.89	2.03
7	0	1	0	4	50	1.5	1.76	0.59
8	0	0	1	4	75	1	1.02	3.05
9	1	–1	–1	6	25	0.5	1.48	1.66
10	0	–1	0	4	50	0.5	2..43	2.91
11	–1	–1	1	2	75	0.5	23.32	23.05
12	1	1	–1	6	25	1.5	2.02	2.46
13	–1	1	–1	2	25	1.5	9.04	10.38
14	0	0	–1	4	25	1	2.49	0.25
15	0	0	0	4	50	1	1.29	1.99
16	0	0	0	4	50	1	1.30	1.99

Table 3. ANOVA results of the RSM-FCCCD model applied to Cr(VI) biosorption onto WAC

Source	Sum of squares	*df*[a]	Mean square	F-value	p-value
Model	855.20	9	95.02	24.59	0.0005
A (=pH)	561.19	1	561.19	145.25	< 0.0001
B (=dose)	13.53	1	13.53	3.50	0.1105
C (=C_0)	26.95	1	26.95	6.98	0.0385
AB	8.42	1	8.42	2.18	0.1904
AC	50.33	1	50.33	13.03	0.0112
BC	2.31	1	2.31	0.5974	0.4689
A^2	149.31	1	149.31	38.64	0.0008
B^2	0.1566	1	0.1566	0.0405	0.8471
C^2	0.9145	1	0.9145	0.2367	0.6439
Residual	23.18	6	3.86		
Lack of Fit	23.18	5	4.64		
Pure Error	0.0000	1	0.0000		
Total Corr	878.38	15			
R^2	0.974				
Adjusted R^2	0.934				
C.V. (%)	21.7				

Note: [a] df – degrees of freedom.

pH, can be in the form of chromate (CrO_4^{2-}), dichromate ($Cr_2O_7^{2-}$) or bichromate ($HCrO_4^-$) (See Fig. 4). Thus, at the pH range 2 to 6, Cr(VI) is mainly as $HCrO_4^-$. At pH below 2, that is under strongly acidic conditions the presence of H^+ protons would drive the reduction process of Cr(VI) to Cr(III), according to Equation 6 (Verma et al., 2021). At this pH range (pH < 2), the fraction of $HCrO_4^-$ decreases, favoring the predominance of neutral H_2CrO_4 (See Fig. 4).

$$HCrO_4^- + 7H^+ + 3e^- \rightarrow Cr^{3+} + 4H_2O \quad (6)$$

Figure 5 shows optimization contours generated using the RSM-FCCCCD model. The maximum

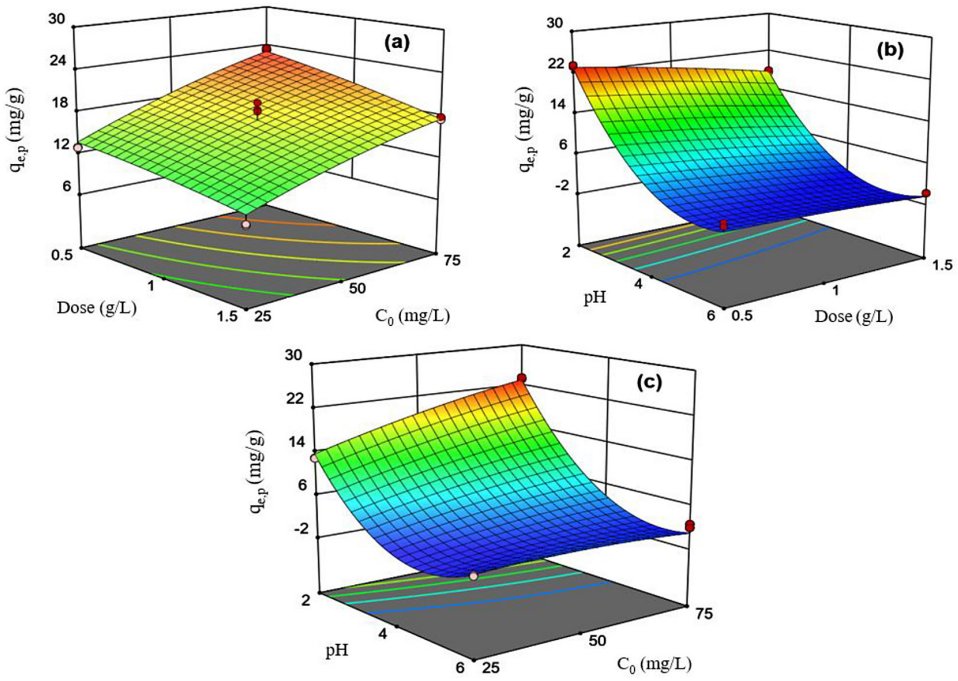

Figure 3. Three-dimensional graphs of: (a) $q_{e,p}$ *vs* dose and C_0; (b) $q_{e,p}$ *vs* dose and pH; (c) $q_{e,p}$ *vs* pH and C_0

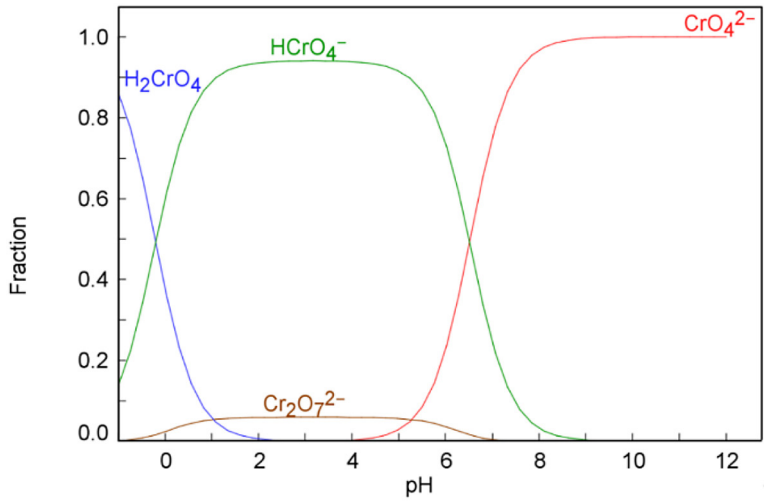

Figure 4. Distribution of chromium species in aqueous media under different pH levels

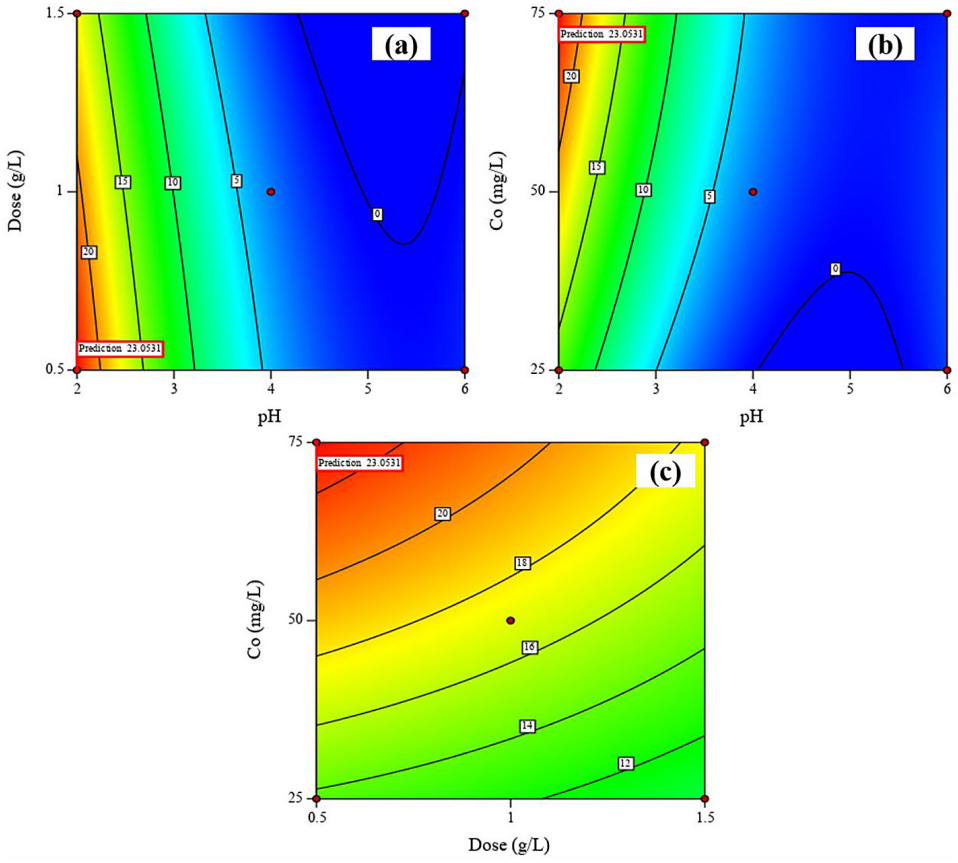

Figure 5. Contour plots of $q_{e,p}$ on (a) dose –pH; (b) C_0 – pH and (c) dose-C_0

predicted adsorption capacity, $q_{e,p,max}$ = 23.38 (23.05) mg/g is obtained from Equation 4 and Equation 5 at the critical intersection points within the red areas: pH 2, C_0 = 75 mg/L and WAC-dose = 0.5 g/L. Our results are consistent with those reported by Li et al. (2023), Kumari et al. (2021) and Lall et al. (2022), who employed biosorbents derived from lignin, coconut residues and *Saraca asoca*, respectively; and observed a maximum q_e at pH 2.

Adsorption isotherm

Adsorption isotherms are crucial tools for characterizing the biosorption process (Musah et al., 2022). The experimental isotherm data (q_e

vs C_e), obtained under optimized operational parameters (dose, pH and C_0) at equilibrium conditions, are very well adjusted by Langmuir and Freundlich and also Temkin models (See Fig. 6), given that the fitted R^2 values are similar to each other (≥ 0.95) (Table 4). This result shows that chromium sorption onto WAC is a favorable process (Kumari et al., 2021; Lavado-Meza et al., 2023b) involving various adsorption mechanisms, such as chemisorption, physisorption, among others (Araújo et al., 2018; Ehiomogue et al., 2022; Musah et al., 2022).

It is interesting to note that the q_{max} = 30.5 mg/g reported in this study (see Table 4) is one of the highest q_{max} values for Cr(VI) removal using similar biosorbents (see Table 5). This capacity is considerably higher than that observed in materials such as orange peel (4.96 mg/g), peanut shell (2.48 mg/g), banana peel (10.2 mg/g), blueberry peel (6.81 mg/g), and potato peel (3.28 mg/g). This finding highlights the potential of WAC as an effective material for the treatment of water contaminated with Cr(VI) ions. In terms of sustainability, WAC offers additional advantages as an abundant, low-cost waste material that can be recycled, contributing to waste reduction and the circular economy. Its high Cr(VI) adsorption capacity makes it suitable for large-scale applications, particularly in coffee-producing regions, making it an attractive option both economically and environmentally.

Reaction kinetics

The kinetic biosorption processes provide crucial information on the time-dependent interactions of the biological material with the aqueous medium. The time evolution of the Cr(VI)

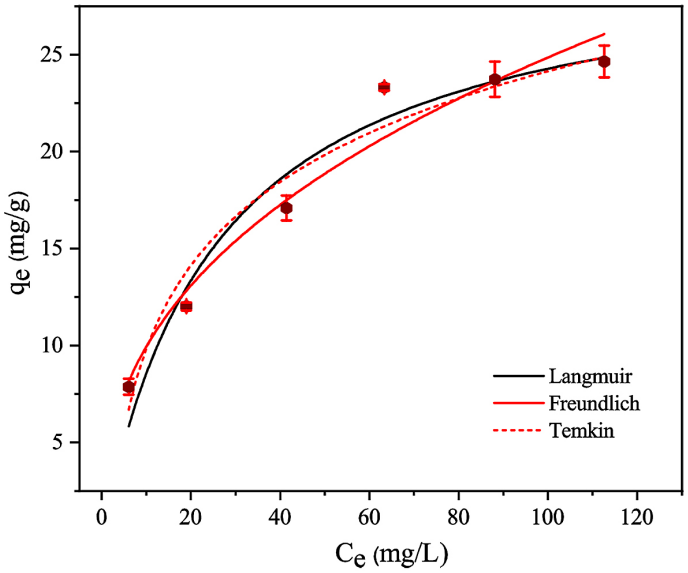

Figure 6. Experimental isotherm data, at T=20 °C, t_{sp} = 120 min

Table 4. Isotherm models applied to Cr(VI) biosorption onto WAC

Isotherm models	Parameters	
Langmuir $q_e = q_{max}\frac{K_L C_e}{1 + K_L C_e}$	q_{max}	30.5 mg/g
	K_L	0.04 L/mg
	R^2	0.96
Freundlich $q_e = K_F C_e^{1/n}$	K_F	3.97 mg/g
	n	2.51
	R^2	0.96
Temkin $q_e = \frac{RT}{B} ln(A_T C_e)$	A_T	0.48 L/g
	B	395.03 J/mol
	R^2	0.95

Table 5. Maximum adsorption capacities, q_{max}, to remove Cr(VI) using biosorbents coming from agriculture waste

Biosorbents	q_{max} (mg/g)	References
Orange peel	4.96	(Khalfaoui et al., 2024)
Leaves (*Sambucus nigra L.*)	6.389	(Mancilla et al., 2022)
Gliricidia sepium Leaf Powder	35.71	(Suganya et al., 2019)
Lagerstroemia speciosa bark	20.40	(Srivastava et al., 2015)
Ficus carica	19.58	(Gupta et al., 2013)
Peanut shells	2.48	(Rzig et al., 2021)
S. glauca	10.9	(Banchhor et al., 2021)
Banana peel; Cranberry kernel shell	10.2; 6.81	(Parlayici and Pehlivan, 2019)
Potatoes peel	3.28	(Mutongo et al., 2014)
Waste Arabica-Coffee (WAC)	30.5	This work

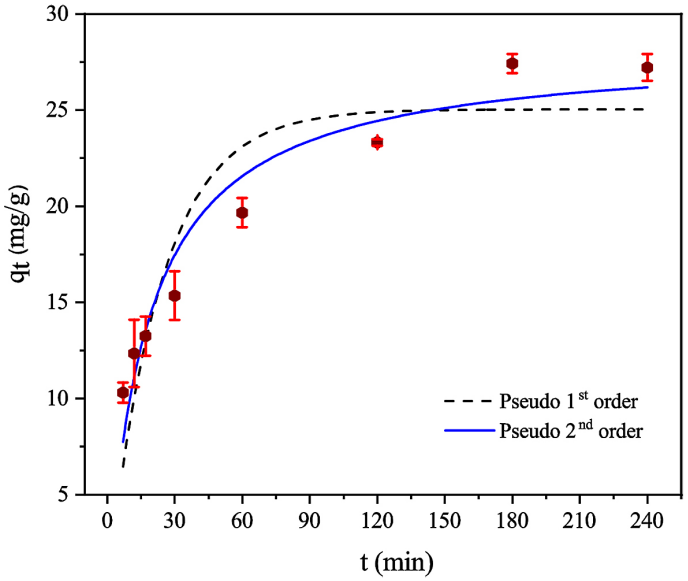

Figure 7. (q_t *vs* t) kinetic experimental data of Cr(VI) biosorption onto WAC at T= 20 °C

biosorption capacity, q_t, was examined under optimized experimental conditions at T= 20 °C (Figs. 7 and 8).

The kinetic experimental data were adjusted to three models: *pseudo*-1st and *pseudo*-2nd-order kinetics, and Webber-Morris-intraparticle-diffusion model. The kinetic constants obtained from non-linear fits are given in Table 6. The (q_t *vs* t) relationship is best adjusted with the *pseudo* 2nd order model (R^2 = 0.93) (Fig. 7), suggesting that Cr(VI) biosorption occurs mainly *via* the chemisorption mechanism (Jaihan et al., 2022). The literature

Table 6. Parameters of kinetic models applied to Cr(VI) biosorption onto WAC

Kinetic models	Kinetic parameters	
Pseudo-1st order $q_t = q_e(1 - e^{-k_1 t})$	q_e	25.04 mg/g
	k_1	0.04 1/min
	R^2	0.84
Pseudo-2nd order $q_t = \frac{{q_e}^2 k_2 \cdot t}{1 + q_e \cdot k_2 \cdot t}$	q_e	22.32 mg/g
	k_2	1.26 g/mg min
	R^2	0.93
Intraparticular diffusion of Webber-Morris $q_t = k_{id} \cdot t^{0.5} + C$	$k_{d\,I}$	1.78 (mg/g) $(1/s)^{0.5}$
	R^2	0.99
	$k_{d\,II}$	1.06 (mg/g) $(1/s)^{0.5}$
	R^2	0.92

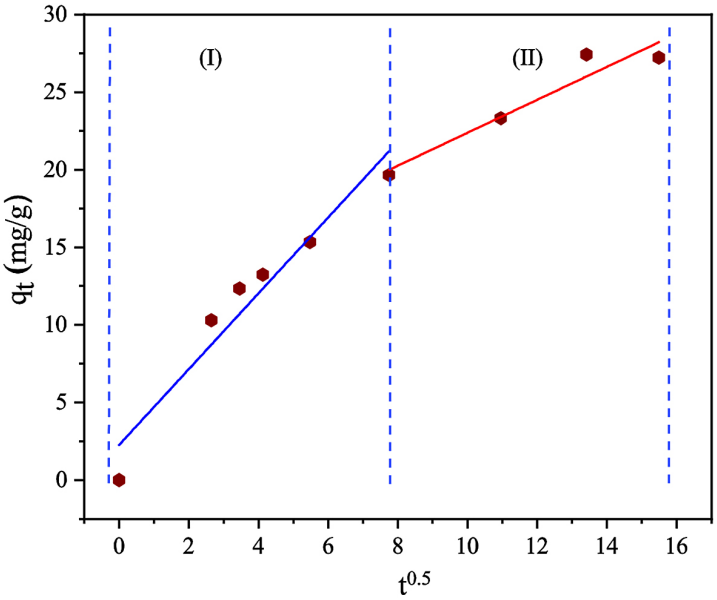

Figure 8. Weber-Morris intraparticle diffusion at T = 20 °C

Table 7. Thermodynamic values of the Cr(VI) biosorption onto WAC

ΔG° (kJ/mol)			ΔH° (kJ/mol)	ΔS° (J/mol K)
296 K	303 K	323 K		
–14.41	–15.31	–17.13	12.15	90.64

reports similar results with other agricultural residues (Boddu et al., 2023; Ren et al., 2022; Srivastava et al., 2015).

In Figure 8, q_t vs $t^{0.5}$ experimental data were fitted to the Webber-Morris intraparticle diffusion model. Two distinct stages in the biosorption process can be identified:

- External diffusion, associated with the transport of hexavalent chromium ions from the aqueous medium to the biomass surface (Pant et al., 2022).
- Internal diffusion, associated with the migration of chromium ionic compounds, from the surface (external boundary layer), through the internal cavities of the biomass (Gupta et al., 2013).

The linear segment of the graphical representation exhibits a non-zero intercept, suggesting that additional kinetic factors beyond pore diffusion control the adsorption rate (Albadarin et al., 2011; Lavado-Meza et al., 2023a; Pant et al., 2022).

Values of thermodynamic functions of the hexavalent chromium biosorption are given in Table 7. We can see that this process is spontaneous ($\Delta G^0 < 0$), endothermic ($\Delta H^0 > 0$) and with increased randomness ($\Delta S^0 > 0$) at the interface of the aqueous medium and the biosorbent surface.

CONCLUSIONS

The RSM-FCCCD methodology allowed us to optimize the Cr(VI) biosorption capacity q_e of Arabica-coffee pulp biomass (WAC), in terms of key factors, such as pH, chromium concentration C_0 and WAC-dose. A quadratic dependence of the predicted Cr(VI) biosorption capacity $q_{e,p}$ was obtained as a function of key-factors, highlighting the strong influence of the pH factor. The optimal values of the considered factors were pH 2, C_0 = 75 mg/L WAC-dose = 0.5g/L. These values were taken into account to obtain a q_{max} = 30.5 mg/g. FTIR analysis of WAC (loaded and unloaded with Cr) showed the presence of OH, CH, CO, COH groups associated among others with cellulose, hemicellulose, lignin and polysaccharides. SEM imaging revealed that the clean WAC exhibited a rough and porous surface morphology, while Cr(VI)-loaded WAC displayed a more compact and less porous surface. Furthermore, the equilibrium relationship (q_e vs C_e) was well adjusted to Langmuir, Freundlich and Temkin isotherm models, indicating that the biosorption mechanism involves complex processes, such as chemisorption, Van der Waals attractions and other interactions;

although chemisorption stands out, given that the kinetic relationship (q_t *vs* t) fits well to the *pseudo*-2nd-order kinetic model. On the other hand, the evaluation of thermodynamic functions showed that the biosorption studied is a spontaneous ($\Delta G^0 < 0$) and endothermic ($\Delta H^0 > 0$) process. Finally, it is important to mention that this work presents an interesting approach to the potential use of coffee processing waste (coffee pulp) as an eco-friendly and low-cost material capable of removing heavy metals, e.g. chromium, from aqueous systems.

REFERENCES

1. Albadarin, A.B., Al-Muhtaseb, A.H., Al-laqtah, N.A., Walker, G.M., Allen, S.J., Ahmad, M.N.M., (2011). Biosorption of toxic chromium from aqueous phase by lignin: mechanism, effect of other metal ions and salts. *Chem. Eng. J. 169*, 20–30. https://doi.org/10.1016/j.cej.2011.02.044
2. Alvarado, C.W., Bobadilla, L.G., Valqui, L., Silva, G., V, V., Valqui-valqui, L., Vigo, C.N., (2022). Characterization of *Coffea arabica* L. parent plants and physicochemical properties of associated soils, *Peru 8.* https://doi.org/10.1016/j.heliyon.2022.e10895
3. Amaku, J.F., Ogundare, S.A., Akpomie, K.G., 2021. *Pentaclethra macrophylla* stem bark extract anchored on functionalized MWCNT-spent molecular sieve nanocomposite for the biosorption of hexavalent chromium MWCNT-spent molecular sieve nanocomposite for the biosorption of. *Int. J. Phytoremediation 0,* 1–10. https://doi.org/10.1080/15226514.2021.1937930
4. Araújo, C.S.T., Almeida, I.L.S., Rezende, H.C., Marcionilio, S.M.L.O., Léon, J.J.L., de Matos, T.N., (2018). Elucidation of mechanism involved in adsorption of Pb(II) onto lobeira fruit (*Solanum lycocarpum*) using langmuir, freundlich and temkin isotherms. *Microchem. J. 137*, 348–354. https://doi.org/10.1016/j.microc.2017.11.009
5. Baby, R., Zobir, M., Zainal, Z., Halim, A., (2023). Preparation of Functionalized Palm Kernel Shell Bio-adsorbent for the treatment of heavy metal-contaminated water. *J. Hazard. Mater. Adv. 10*, 100253. https://doi.org/10.1016/j.hazadv.2023.100253
6. Ballesteros, L.F., Teixeira, J.A., Mussatto, S.I., (2014). *Chemical, Functional, and Structural Properties of Spent Coffee Grounds and Coffee Silverskin.* https://doi.org/10.1007/s11947-014-1349-z
7. Banchhor, A., Pandey, M., Pandey, P.K., (2021). Optimization of adsorption parameters for effective removal of hexavalent chromium using simarouba glauca from aqueous solution. *Water Conserv. Sci. Eng. 6*, 127–144. https://doi.org/10.1007/s41101-021-00106-z
8. Bayuo, J., Abukari, M.A., Pelig-Ba, K.B., (2020). Optimization using central composite design (CCD) of response surface methodology (RSM) for biosorption of hexavalent chromium from aqueous media. *Appl. Water Sci. 10*. https://doi.org/10.1007/s13201-020-01213-3
9. Ben Khalifa, E., Rzig, B., Chakroun, R., Nouagui, H., Hamrouni, B., (2019). Application of response surface methodology for chromium removal by adsorption on low-cost biosorbent. *Chemom. Intell. Lab. Syst. 189*, 18–26. https://doi.org/10.1016/j.chemolab.2019.03.014
10. Bhattarai, K.P., Pant, B.D., Rai, R., Aryal, R.L., Paudyal, H., Gautam, S.K., Ghimire, K.N., Pokhrel, M.R., Poudel, B.R., (2022). Efficient sequestration of Cr(VI) from aqueous solution using biosorbent derived from Arundo donax stem. *J. Chem. 12.* https://doi.org/10.1155/2022/9926391
11. Boddu, S., Narayana Alugunulla, V., Babu Dulla, J., Ali Khan, A., Babu Kolimarla, B., Jajula, S., (2023). Enhanced biosorption of Cr(VI) from contaminated water using biodegradable natural polymeric biosorbent. *Mater. Today Proc. 72*, 441–450. https://doi.org/10.1016/j.matpr.2022.08.312
12. Castillo, N.E.T., Sierra, J.S.O., Oyervides-mu, M.A., Sosa-hern, J.E., Iqbal, M.N., Parra-saldívar, R., Melchor-martínez, E.M., (2021). Exploring the potential of coffee husk as caffeine bio-adsorbent – A mini-review. *Case Studies in Chemical and Environmental Engineering 3*. https://doi.org/10.1016/j.cscee.2020.100070
13. Collazo-Bigliardi, S., Ortega-toro, R., Chiralt, A., (2019). Using lignocellulosic fractions of co ff ee husk to improve properties of compatibilised starch-PLA blend fi lms. *Food Packag. Shelf Life 22*, 100423. https://doi.org/10.1016/j.fpsl.2019.100423
14. Datt, B., Neupane, D., Ram, D., Chandra, P., Kumar, S., Raj, M., Raj, B., (2022). Efficient biosorption of hexavalent chromium from water by modi fi ed arecanut leaf sheath 8. *Helyion.* https://doi.org/10.1016/j.heliyon.2022.e09283
15. Dev, A.M., Unni, A., Mathew, A., Mathew, M., Bhagya, S., Joseph, A., (2024). An evaluation on the prospective application of lignocellulose based biosorbents for the separation of Cr(VI) from aqueous solution : A critical review. *Sep. Sci. Technol*. 1–23. https://doi.org/10.1080/01496395.2024.2371370
16. Ehiomogue, P., Ahuchaogu, I.I., Ahaneku, I.E., (2022). Review of adsorption isotherms models. *Acta Tech. Corviniensis 14*, 87–96.
17. Freitas, V.V., Borges, L.L.R., Vidigal, M.C.T.R., dos Santos, M.H., Stringheta, P.C., (2024). Coffee: A comprehensive overview of origin, market, and the quality process. *Trends Food Sci. Technol. 146*, 104411. https://doi.org/10.1016/j.tifs.2024.104411

18. Gupta, V.K., Pathania, D., Agarwal, S., Sharma, S., 2013. Removal of Cr(VI) onto Ficus carica biosorbent from water. *Environ. Sci. Pollut. Res. 20*, 2632–2644. https://doi.org/10.1007/s11356-012-1176-6
19. Jaihan, W., Mohdee, V., Sanongraj, S., Pancharoen, U., Nootong, K., (2022). Biosorption of lead (II) from aqueous solution using Cellulose-based Bioadsorbents prepared from unripe papaya (Carica papaya) peel waste: Removal Efficiency, Thermodynamics, kinetics and isotherm analysis. *Arab. J. Chem. 15,* 103883. https://doi.org/10.1016/j.arabjc.2022.103883
20. Jimenez-Paz, J., Lozada-castro, J.J., Lester, E., Williams, O., Stevens, L., (2023). Solutions to Hazardous Wastes Issues in the Leather Industry: Adsorption of Chromium III and VI from Leather Industry Wastewaters using Activated Carbons Produced from Leather Industry Solid Wastes. *J. Environ. Chem. Eng.* 109715. https://doi.org/10.1016/j.jece.2023.109715
21. Khalfaoui, A., Benalia, A., Selama, Z., Hammoud, A., Derbal, K., Panico, A., Pizzi, A., (2024). Removal of chromium(VI) from water using Orange peel as the biosorbent: Experimental, modeling, and kinetic studies on adsorption isotherms and chemical structure. *Water 16*, 742. https://doi.org/10.3390/w16050742
22. Kumari, B., Tiwary, R.K., Yadav, M., Singh, K.M.P., (2021). Nonlinear regression analysis and response surface modeling of Cr(VI) removal from synthetic wastewater by an agro-waste Cocos nucifera: box-behnken design (BBD). *Int. J. Phytoremediation 23*, 791–808. https://doi.org/10.1080/15226514.2020.1858399
23. Lala, M.A., Ntamu, T.E., Adesina, O.A., Popoola, L.T., Yusuff, A.S., Adeyi, A.A., (2023). Adsorption of hexavalent chromium from aqueous solution using cationic modified rice husk : Parametric optimization via Taguchi design approach Adsorption of hexavalent chromium from aqueous solution using cationic modified rice husk : Parametric optimiza. *Scientific African 20*. https://doi.org/10.1016/j.sciaf.2023.e01633
24. Lall, A.S., Pandey, A.K., Mani, J.V., 2022. Biosorption potential of saraca asoca bark powder for removal of Cr (VI) ions from aqueous solution. *Pollution 8*, 249–267. https://doi.org/10.22059/POLL.2021.329212.1164
25. Lavado-Meza, C., De la Cruz-Cerrón, L., Asencios, Y.J.O., Marcos, F.C.F., Dávalos-Prado, J.Z., (2023a). Alkaline modification of arabica-coffee and theobroma-cocoa agroindustrial waste for effective removal of Pb(II) from aqueous solutions. *Molecules 28*, 683. https://doi.org/10.3390/molecules28020683
26. Lavado-Meza, C., De la Cruz-Cerrón, L., Cisneros-Santos, G., De la Cruz, A.H., Angeles-Suazo, J., Dávalos-Prado, J.Z., (2023b). Arabica-coffee and teobroma-cocoa agro-industrial waste biosorbents, for Pb(II) removal in aqueous solutions. *Environ. Sci. Pollut. Res. 30*, 2991–3001. https://doi.org/10.1007/s11356-022-22233-3
27. Li, L., Cao, G., Zhu, R., (2021). Adsorption of Cr(VI) from aqueous solution by a litchi shell-based adsorbent. *Environ. Res. 196*, 110356. https://doi.org/10.1016/j.envres.2020.110356
28. Li, W., Chai, L., Du, B., Chen, X., Sun, R.C., (2023). Full-Lignin-Based adsorbent for removal of Cr(VI) from waste water. *Sep. Purif. Technol. 306.* https://doi.org/10.1016/j.seppur.2022.122644
29. Lu, M., Fang, S., Li, G., Wang, W., Tan, X., Wu, W., (2023). Optimization of adsorption performance of cerium-loaded intercalated bentonite by CCD-RSM and GA-BPNN and its application in simultaneous removal of phosphorus and ammonia nitrogen. *Chemosphere 336*, 139241. https://doi.org/10.1016/j.chemosphere.2023.139241
30. Mahmoud, A.E.D., Fawzy, M., Hosny, G., Obaid, A., (2020). Equilibrium, kinetic, and diffusion models of chromium(VI) removal using *Phragmites australis* and *Ziziphus spina*-christi biomass. *Int. J. Environ. Sci. Technol. 18*, 2125–2136. https://doi.org/10.1007/s13762-020-02968-7
31. Mancilla, H.B., Cerrón, M.R., Aroni, P.G., Paucar, J.E.P., Tovar, C.T., Jindal, M.K., Gowrisankar, G., (2022). Effective removal of Cr (VI) ions using low-cost biomass leaves (*Sambucus nigra* L.) in aqueous solution. *Environ. Sci. Pollut. Res. 30*, 106982–106995. https://doi.org/10.1007/s11356-022-24064-8
32. Matouq, M., Saleh, M., Al-Ayed, O., El-Hasan, T., Hiroshi, Y., Tagawa, T., (2021). Biosorption of chromium and nickel from aqueous solution using pine cones, eucalyptus bark, and moringa pods: A comparative study. *Water Pract. Technol. 16*, 72–82. https://doi.org/10.2166/wpt.2020.096
33. Murthy, T.P.K., Gowrishankar, B.S., (2020). Process optimisation of methylene blue sequestration onto physical and chemical treated coffee husk based adsorbent. *SN Appl. Sci. 2*, 1–18. https://doi.org/10.1007/s42452-020-2603-9
34. Musah, M., Azeh, Y., Mathew, J., Umar, M., Abdulhamid, Z., Muhammad, A., (2022). Adsorption kinetics and isotherm models : A review. *CaJoST 4*, 20–26. https://doi.org/10.4314/cajost.v4i1.3
35. Mutongo, F., Kuipa, O., Kuipa, P.K., (2014). Removal of Cr(VI) from aqueous solutions using powder of potato peelings as a low cost sorbent. *Bioinorg. Chem. Appl.* https://doi.org/10.1155/2014/973153
36. Najafpour, A., Rajabi Khorrami, A., Aberoomand Azar, P., Saber Tehrani, M., (2020). Study of heavy metals biosorption by tea fungus in Kombucha drink

using Central Composite Design. *J. Food Compos. Anal. 86*, 103359. https://doi.org/10.1016/j.jfca.2019.103359

37. Nasir, Z., Sabir, A., Muhammad, H., (2023). Fingerprinting of heavy metal and microbial contamination uncovers the unprecedented scale of water pollution and its implication on human health around transboundary Hudiara drain in South Asia. *Environ. Technol. Innov. 30*, 103040. https://doi.org/10.1016/j.eti.2023.103040
38. Pant, B.D., Neupane, D., Paudel, D., Lohani, C., Gautam, S., Pokhrel, M., Poudel, B., (2022). Efficient biosorption of hexavalent chromium from water by modified arecanut leaf sheath. *Heliyon 8*. https://doi.org/10.1016/j.heliyon.2022.e09283
39. Parlayici, Ş., Pehlivan, E., (2019). Comparative study of Cr(VI) removal by bio-waste adsorbents: equilibrium, kinetics, and thermodynamic. *J. Anal. Sci. Technol. 10*, 15. https://doi.org/10.1186/s40543-019-0175-3
40. Pérez, L., Paz, I., Sandoval, A., Peñaloza, G., (2020). Uso de cáscara de cacao (*Theobroma cacao*) para la remocion de cromo en solución acuosa. *Rev. EIA 17*, 1–13. https://doi.org/10.24050/reia.v17i34.1393
41. Ren, B., Jin, Y., zhao, L., Cui, C., Song, X., (2022). Enhanced Cr(VI) adsorption using chemically modified dormant Aspergillus niger spores: Process and mechanisms. *J. Environ. Chem. Eng. 10*, 106955. https://doi.org/10.1016/j.jece.2021.106955
42. Rzig, B., Guesmi, F., Sillanpää, M., Hamrouni, B., (2021). Modelling and optimization of hexavalent chromium removal from aqueous solution by adsorption on low-cost agricultural waste biomass using response surface methodological approach. *Water Sci. Technol. 84*, 552–575. https://doi.org/10.2166/wst.2021.233
43. Senanu, L.D., Kranjac-berisavljevic, G., Cobbina, S.J., (2023). The use of local materials to remove heavy metals for household-scale drinking water treatment : A review. *Environ. Technol. Innov. 29*, 103005. https://doi.org/10.1016/j.eti.2023.103005
44. Shan, R., Shi, Y., Gu, J., Bi, J., Yuan, H., Luo, B., (2020). Aqueous Cr (VI) removal by biochar derived from waste mangosteen shells : Role of pyrolysis and modi fi cation on its absorption process. *J. Environ. Chem. Eng. 8*, 103885. https://doi.org/10.1016/j.jece.2020.103885
45. Singh, R., Bhateria, R., (2020). Optimization and experimental design of the Pb 2 + adsorption process on a Nano-Fe_3O_4 - Based adsorbent using the response surface methodology. https://doi.org/10.1021/acsomega.0c04284
46. Solis, A., Roy, R., Golsztajn, A., Tavares, J.R., Dumont, M., (2023). Selective adsorption of Cr (III) over Cr (VI) by starch-graft-itaconic acid hydrogels. *J. Hazard. Mater. Adv. 10*, 100255. https://doi.org/10.1016/j.hazadv.2023.100255
47. Soon, W.L., Peydayesh, M., Mezzenga, R., Miserez, A., (2022). Plant-based amyloids from food waste for removal of heavy metals from contaminated water. *Chem. Eng. J. 445*, 136513. https://doi.org/10.1016/j.cej.2022.136513
48. Srivastava, S., Agrawal, S.B., Mondal, M.K., (2015). Biosorption isotherms and kinetics on removal of Cr(VI) using native and chemically modified Lagerstroemia speciosa bark. *Ecol. Eng. 85*, 56–66. https://doi.org/10.1016/j.ecoleng.2015.10.011
49. Suganya, E., Saranya, N., Patra, C., Varghese, L.A., Selvaraju, N., (2019). Biosorption potential of Gliricidia sepium leaf powder to sequester hexavalent chromium from synthetic aqueous solution. *J. Environ. Chem. Eng. 7*, 103112. https://doi.org/10.1016/j.jece.2019.103112
50. Tejada, C., Paz, I., Acevedo, D., Espinosa, M., López, C., (2020). Adsorption of chrome (VI) and mercury (II) in solution using hyacinth (*Eichhornia crassipes*). Biotecnol. en el Sect. *Agropecu. y Agroindustrial 19*, 54–65. https://doi.org/10.18684/BSAA(19)54-65
51. Thakur, L.S., Baghel, R., Sharma, A., Sharma, S., Verma, S., Parmar, H., Kumar Varma, A., Mondal, P., (2023). Simultaneous removal of lead, chromium and cadmium from synthetic water by electrocoagulation: Optimization through response surface methodology. *Mater. Today Proc. 72*, 2697–2704. https://doi.org/10.1016/j.matpr.2022.09.031
52. Thangagiri, B., Sakthivel, A., Jeyasubramanian, K., Seenivasan, S., Raja, J.D., (2022). Removal of hexavalent chromium by biochar derived from Azadirachta indica leaves : Batch and column studies. *Chemosphere 286*, 131598. https://doi.org/10.1016/j.chemosphere.2021.131598
53. Verma, R., Maji, P., Sarkar, S., (2021). Comprehensive investigation of the mechanism for Cr(VI) removal from contaminated water using coconut husk as a biosorbent. *J. Clean. Prod. 314*. https://doi.org/10.1016/j.jclepro.2021.128117
54. Wang, H., Wang, W., Zhou, S., Gao, X., (2023). Adsorption mechanism of Cr(VI) on woody-activated carbons. *Heliyon 9*, e13267. https://doi.org/10.1016/j.heliyon.2023.e13267
55. Yusuff, A.S., Ishola, N.B., Gbadamosi, A.O., Epelle, E.I., (2023). Modeling and optimization of hexavalent chromium adsorption by activated eucalyptus biochar using response surface methodology and adaptive neuro-fuzzy inference system. *Environments 10*, 55. https://doi.org/10.3390/environments10030055